Available online at www.sciencedirect.com
SCIENCE DIRECT®
Journal of Hydrology 283 (2003) 41–56
Journal of Hydrology
www.elsevier.com/locate/jhydrol

Land-surface hydrological processes in the permafrost region of the eastern Tibetan Plateau

Yinsheng Zhang[a,*], T. Ohata[a,b], T. Kadota[a]

[a]*Frontier Observational Research System for Global Change, Institute for Global Change Research, 3171-25, Showa-cho, Kanazawa-ku, Kanagawa 236-0001, Japan*
[b]*Institute for Low Temperature Science, Hokkaido University, Sapporo, Japan*

Received 2 January 2002; accepted 23 June 2003

Abstract

In order to examine and record the effects of permafrost on hydrological processes in the cryosphere, the hydrology of the ground surface layer was investigated in the permafrost region of the eastern Tibetan Plateau. Water budget components in the surface layer were calculated on a daily basis. Variability in the water budget components, and its causes, was investigated on both seasonal and daily bases. The results showed that coupling of the thaw–frost cycle to seasonality in precipitation is the principal control of hydrological processes in the upper 2 m of the soil. When the ground surface begins to thaw, from the surface down, the concentration of melt water within a thin surface layer leads to a rapid increase in evaporation, then a slight decrease occurs in the continuous permafrost region as the wet soil zone moves downward. An analysis of seasonal variation in the water budget components demonstrated that the dominant water cycling arises from the processes of precipitation and evaporation that are typical in this region. The freeze–thaw cycle, which affects seasonal soil moisture, water storage, evaporation, and the mobilization of water through the soil and vegetation during the summer monsoon season, is a dominant feature of the land-surface hydrology in the permafrost region of the eastern Tibetan Plateau.

Keywords: Tibetan Plateau; Permafrost; Ground surface layer; Water budget; Hydrological process

1. Introduction

The cryosphere, one of the first regions to show the effects of the increasing human impact on climate systems, consists of ice in all its forms, permafrost, snow cover and glaciers. Cryospheric observations provide quite unequivocal evidence of 20th century atmospheric warming. There is an increasing awareness that the cryosphere plays a significant role in the interannual variability of the climatic system, and of its impact on vitally important water resources (Kukla and Kukla, 1974; Williams, 1975; Hahn and Shukla, 1976; Barnett et al., 1988; Lawford, 1993). The cryosphere is a heat sink for the atmosphere, making it an important element that controls the water cycle and heat budget in the atmosphere–hydrosphere system.

The Tibetan Plateau, the most important example of a high-altitude cryosphere, is sensitive to global

* Corresponding author.
E-mail address: yszhang@jamstec.go.jp (Y. Zhang).

0022-1694/$ - see front matter © 2003 Elsevier B.V. All rights reserved.
doi:10.1016/S0022-1694(03)00240-3

warming. Energy and water cycles over the Tibetan Plateau play an important role in the Asian Monsoon system, which in turn is a major component of both the energy and water cycles of the global climate. Of particular importance is the melt season, when snowmelt and evaporation occur simultaneously, but in different parts of the region. Through its effects on hydrology, the presence of permafrost increases the complexities of land-surface hydrological processes through contrasting thermal and water regimes in the ground. Differential heating and evaporation, together with advection, are amplified by the hydrology of the permafrost terrain.

The response of land surface processes to atmospheric forcing, and its feedback, has become a prominent, important subject in the quest to better understand global and regional water cycles. Therefore, land-surface hydrological processes on the Tibetan Plateau need to be documented in detail to better understand the Asian monsoon system. For this purpose, great effort must be focused on permafrost regions because land-surface hydrological processes are very involved and complicated. A unique, important feature of land-surface hydrology in these regions, associated with the long, cold winter, is the presence of permafrost and an active summer layer (the layer of soil above the permafrost that thaws each summer). Permafrost limits the amount of subsurface water storage and infiltration that can occur, leading to wet soils and ponded surface water, which might be thought unusual for a region with such limited precipitation. The thickness of the active layer and its permafrost condition are largely controlled by surface heat fluxes, which couple the hydrology to the surface energy budget so closely that they cannot be quantified separately. In summer, solar heating leads to rapid thawing of the active layer, while in winter, a delicate balance between the thermal insulation of snow cover and its high albedo controls the rate and severity of freezing.

There is growing research on permafrost hydrology, e.g. hydrological research in the Mackenzie GEWEX (Rouse, 2000). The role of permafrost in subarctic hydrology has been examined in wetlands in North America (Woo and Winter, 1993; Woo and Xia, 1996). Carey and Woo (1999) addressed the seasonal pattern of hydrological processes in a subarctic catchment by comparing the water budget components on two forested slopes, one of which was underlain by permafrost. A process-based, spatially distributed hydrological model was developed for the Arctic and applied in northern Alaska (Zhang et al., 2000). Observations of components of the hydrologic cycle, including precipitation, discharge, soil wetness, and ground surface meteorology conditions, have been carried out for several years on the central Tibetan Plateau under the auspices of the GAME/Tibet project (Koike, 2000). The heat and water fluxes have been calculated at several locations (Tanaka et al., 2001); hydrological processes were investigated using a hydrologic model and large-scale data analysis (Nagai et al., 2002). Simultaneously, the atmospheric processes over the permafrost were documented, but the study of hydrologic processes in the ground and their impact on the water cycle remains incomplete. This paper examined hydrologic processes in the ground surface layer and their impact on the water cycle using data from the GEWEX Asian Monsoon Experiment (GAME)/Tibet Pre-phase Observation Period (POP) 97 and Intensive Observation Period (IOP) 98.

2. Study region, data and calculation

2.1. Studying region

Table 1 gives details on the sites where the data we analyzed were collected. They are all located within the region covered by the GAME/Tibet Project. The sites at D66, Tuotuohe and Amdo are located in areas of spatially continuous permafrost, where the maximum thawing front can reach a depth of 3.0 m. D66 is located in a rather dry region, where less than 120 mm of precipitation was recorded from May to September 1998; in the hydrological year September 1, 1997 to August 31, 1998, the observed annual mean air temperature, relative humidity and wind speed were -6.3 °C, 58% and 3.5 m/s, respectively. Sandy soil with some organic components to a depth of 2 m is found at the site, and is related to the rather sparse vegetation of desert steppe (Zhou et al., 2000).

Table 1
The observation sites and their surface condition

Station	Location	Elevation (m a.s.l.)	Ground surface conditions
D66	35°52′N, 93°78′E	4600	Sparse grass
Tuotuohe	34°13′N, 92°26′E	4353	Sparse grass
Amdo	32°15′N, 91°38′E	4700	Grass land
MS3608	31°14′N, 91°47′E	4610	Range land

The topography is very flat and no streams or lakes are visible from the study site.

The Tuotuohe site is also located in a dry region. Based on records from 1957 to 1998, the mean annual precipitation was 275.5 mm, with about 92% occurring in the summer (May–September); the mean air temperature, relative humidity, and wind speed were −4.3 °C, 57% and 2.5 m/s, respectively. The vegetation cover and soil conditions at Tuotuohe are the same as at D66, and are characterized by sandy soil and sparse, very short vegetation; the maximum height of the grass is less than 5 cm (Zhou et al., 2000). The Tuotuohe River is 300 m north of the study site.

The Amdo site is located in the Amdo River basin, near the Tanggula Pass. The basin valley is not large, but the location of the study site is very flat. A seasonal stream is located in the valley, about 600 m from the site. The ground surface is essentially bare soil in the pre-monsoon dry season, but is covered with scattered short grasses during the summer monsoon season. At the beginning of the monsoon season (late May), the water table is present on the ground. The main vegetation is Stipa glareosa, with 10–50% coverage. Due to the denser vegetation cover, more organic material was found at Amdo than at D66 or Tuotuohe (Tanaka et al., 2001). The annual precipitation from September 1, 1997 to August 31, 1998 was 346.7 mm. In the summer monsoon season (May–September), the mean air temperature, relative humidity, and wind speed were 6.8 °C, 63% and 3.3 m/s, respectively.

The most southerly site, MS3608, is located in a region with discontinuous permafrost. The typical hummocky microtopography of permafrost country is not present near this site. However, the water table was present on the ground at the beginning of the monsoon season (late May). The Naqu River is 10 km south of the study site. The vegetation here is more developed than at the other three sites; the maximum height can reach 30 cm with 60–80% coverage. Meadow soil with abundant organic material in the surface layer has been reported near the study site (Zhou et al., 2000). The summer mean (May–September) air temperature, relative humidity, and wind speed were 8.9 °C, 67% and 3.2 m/s, respectively. In the hydrological year September 1, 1997 to August 31, 1998, the precipitation was 616.2 mm, of which more than 90% occurred during the summer monsoon season.

2.2. Data

The data from all the sites, collected as part of GAME/Tibet POP in 1997 and IOP in 1998, were obtained using three observation systems: an automatic weather station (AWS), a soil moisture and temperature monitoring system (SMTMS), and a precipitation gauge. The parameters measured by the AWS included air temperature (T_a), wind speed (U), air pressure (P), relative humidity (R_h), and ground surface temperature (T_s). The SMTMS measured the volumetric soil water content (θ) and soil temperature (T_g) at several depths. Some of the precipitation data (P_r) from a nearby meteorological station were used to extend the data series. Details of the installations and periods of record are shown in Table 2.

Here, the data on θ need to be explained in more detail. In this work, θ denotes the volumetric soil water content relative to the total volume of soil including dry matter. When the soil temperature exceeds 0 °C, θ denotes the volumetric soil liquid water content, which can be calculated from the TDR data. When the soil temperature is below 0 °C, θ equals the volumetric soil liquid plus the solid water (ice) content, which was assumed to be the same as that observed the preceding fall just before the soil froze, as long as there was no significant change in the TDR data. While the soil thawed and froze, both liquid and solid water could exist within a layer. θ was calculated as the weighted average according to the thaw/freeze depth. The same method was applied in the permafrost region of eastern Siberia (Sugimoto

Table 2
Summary of the data for the study sites

Observation parameters	Sensor (accuracy)	Installation	Record period			
			D66	Tuotuohe	Amdo	MS3608
Air temperature (T_a)	HMP35A (0.1 °C)	6 m above the ground	Aug 1997–Jun 1998	Aug 1997–Sep	May–Sep 1998	Apr–Sep 1998
Wind speed (U)	OGASAWARA (0.1 m/s)	1.5 m above ground	Aug 1997–Jun 1998	Aug 1997–Sep	May–Sep 1998	Apr–Sep 1998
Up-and down-ward radiation (Q)	EKO MS-402 (7 W m^{-2})	1.5 m above ground	Aug 1997–Jun 1998	Aug 1997–Sep	May–Sep 1998	Apr–Sep 1998
Air pressure (P)	PTB100 0.1 hPa)	1.5 m above ground	Aug 1997–Jun 1998	Aug 1997–Sep	May–Sep 1998	Apr–Sep 1998
Relative humidity (R_h)	HMP35A (1.5%)	1.5 m above ground	Aug 1997–Jun 1998	Aug 1997–Sep	May–Sep 1998	Apr–Sep 1998
Ground surface temperature (T_s)	Infrared Thermometer (<0.5 °C)	Ground surface	Aug 1997–Sep 1998	Aug 1997–Sep	May–Sep 1998	Apr–Sep 1998
Soil volumetric water content (θ)	TDR-probe (1–2%)	Under ground 0.04, 0.2, 0.6, 1.0, 1.6, 1.96 (2.25, 2.58)[a]	Aug 1997–Sep 1998	Aug 1997–Sep 1998	Aug 1997–Sep 1998	Aug 1997–Sep 1998
Soil temperature (T_g)	Pt-100 (0.1 °C)	Under ground 0.04, 0.2, 0.4, 0.6, 0.8, 1.0, 1.3, 1.6, 2.0, 2.42 (2.5, 2.79)[a]	Aug 1997–Sep 1998	Aug 1997–Sep 1998	Aug 1997–Sep 1998	Aug 1997–Sep 1998
Precipitation (P_r)	Weighting-type (0.1 mm)		May–Aug 1998	Aug 1997–Sep 1998	Aug 1997–Sep 1998	Aug 1997–Sep 1998

[a] The greatest depth differed with the site.

et al., 2001). However, it is impossible to ascertain the accuracy of this correction due to a lack of detailed measurements. Comparison of the original and corrected soil moisture data shows a significant difference in winter at every depth (Fig. 1), and the difference was bigger both at the surface and the deepest depth, while it was smaller in the intermediate layer. This difference could be due to the ice content.

2.3. Calculation

The water budget in the soil from ground surface to a given depth can be expressed as

$$\Delta W = P_r - E - \Delta S - (WF_H + WF_V) \quad (1)$$

where P_r is precipitation (mm), E is evapotranspiration (mm), WF_H is the net lateral water flux, which was assumed to be zero in this study because we could not investigate it due to the lack of a reference observation site nearby, WF_V is the vertical water flux in the deepest soil layer studied, and ΔW is the water storage change in the surface soil layer (mm), whichs can be written as $\Delta W = \Delta W_L + \Delta W_S$, where subscripts L and S denote liquid and solid water, respectively.

ΔS is the water storage change related to snow cover (mm), and can be written as $\Delta S = \Delta S_C + \Delta S_M$, where subscripts C and M denote snow accumulation and melt, respectively. Due to the low, intermittent precipitation in the non-monsoon season, the snow cover on the eastern Tibetan Plateau is irregular and is discontinuously distributed over the ground surface, even in the middle of winter. Sato (2001) reported that the maximum snow depth and water equivalent in the study region were 9 cm and 20 mm, respectively, in the period 1993–1998. The snow cover did not last long during this period and the longest period of snow

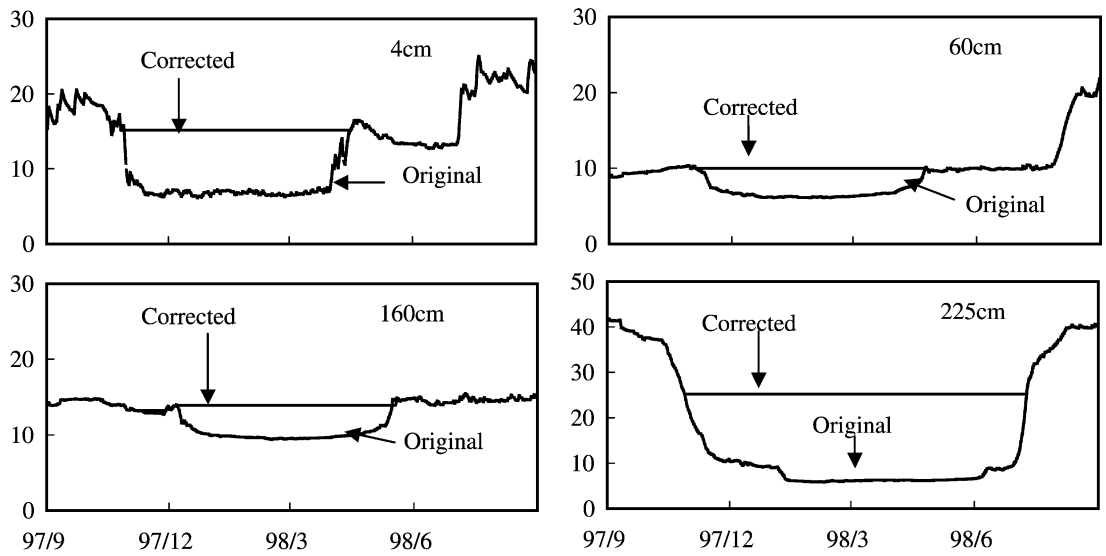

Fig. 1. Comparison of the original soil moisture data measured by TDR and the corrected value for the Tuotuohe site.

cover was about one month in the winter of 1997/98. Additionally, there are no snow depth records in the National Climatic Data Center (NCDC) database. Therefore, the snow cover is considered negligible in the study region. E is computed using the bulk formula (Li et al., 2001)

$$E = \rho\beta C_E U(q_0 - q) \tag{2}$$

where ρ is air density, U is wind speed, q_0 and q are the saturated specific humidity of the land surface and the observed specific humidity of the atmosphere, respectively, β is a parameter determined by the surface soil water content, which can be defined as (Stone and Quirr, 1977)

$$\beta = \frac{\theta_l - \theta_{ec}}{\theta_{sat} - \theta_{ec}} \tag{3}$$

where θ_l is the mean measured soil liquid water content averaged from two layers, θ_{ec} is a criterion for meeting the demands of soil evaporation, which is determined by the soil moisture data when the soil is close to freezing, and has been deduced to range from 6.51 to 8.97% for the Tibetan Plateau. θ_{sat} is the saturated soil moisture, and has been deduced to range from 33 to 37% for the Tibetan Plateau (Li et al., 2001). When the ground surface was frozen, θ_l was determined from the water content TDR measured at the time of the calculation and the preceding fall just before the soil froze, as mentioned in Section 2.2. C_E is the bulk vapor transfer coefficient, which can be calculated from (Brutsaert, 1984)

$$C_E = k^2\left[\ln\left(\frac{z}{z_0}\right) - \Psi_w\right]^{-1}\left[\ln\left(\frac{z}{z_0}\right) - \Psi_m\right]^{-1} \tag{4}$$

where k is the Kármán constant (0.4), z and z_0 are height and roughness, respectively, and Ψ_w and Ψ_m are stratification functions that depend on atmospheric stability.

To calculate ΔW, the ground surface layer is divided into several sublayers at 10 cm intervals. The water content, θ, is calculated at the middle of each layer, using the soil water content profile from SMTMS. The water contained in all the layers at time t can be derived as

$$W_t = \frac{\sum \vartheta_i h_i}{H} \tag{5}$$

where H is the depth of the layer. According to the depth at which the SMTMS sensors were installed, the values of H are taken to be 200 cm at D66, Tuotuohe, Amdo, and 190 cm at MS3608. Therefore, the water storage changes in a given period can be

expressed as:

$$\Delta W = \sum (W_{t+1} - W_t) \tag{6}$$

The vertical water flux at a depth of $H(\mathrm{WF_V})$ is determined by the gradient of the soil-water potential (Kondo and Xu, 1996)

$$\mathrm{WF_V} = -\rho_w k_w \left(\frac{\partial \phi}{\partial z} + 1 \right) \tag{7}$$

where ϕ is the soil-water potential, ρ_w is the water density, k_w is the hydraulic conductivity, and f is the sum of the matric and gravity potentials. The latter is equal to depth $-z$; the matric potential is a function of the volumetric water content (θ) of the form $a \exp(b\theta)$ (Liu and Wang, 1999), where the coefficients a and b are determined from an empirical relationship between the matric potential and volumetric water content applicable to the Tibetan Plateau, originally derived for water and heat balance estimation (Xu and Haginoya, 2001). The calculation of k_w follows the work of Kondo and Xu (1996). $\mathrm{WF_V}$ was calculated at the bottom of the study layer (H), and was assumed to be zero when the soil was frozen. The TDR data, measured at depths of 160 and 225 cm at D66 and Tuotuohe, 160 and 258 cm at Amdo, and 160 and 196 cm at MS3608, were used to estimate the soil water potential gradient.

3. Result of calculation

3.1. Soil thermal/water regime

Fig. 2 shows graphs of soil temperatures at the study sites from September 1997 to August 1998, within the layer from the surface to a depth of 250 cm. The ground thawing process showed similar features at all four sites, starting at the surface in April and rapidly extending to the deeper layers. The thawing front reached 100 cm in early May and 200 cm in mid or late May. At D66 and Tuotuohe, both of which are locate north of study region with colder summer, the increase in soil temperature slowed after June. This tendency was not seen at the other two sites, which locate southern and have relatively high air temperature. In the summer of 1998 (June–August), air temperature were averaged to be 4.2, 6.8, 8.1 and 10.4 at D66, Tuotuohe, Amdo and MS3608 site, respectively.

The ground surface of all four sites started to freeze in late October. Freezing extended deeper more

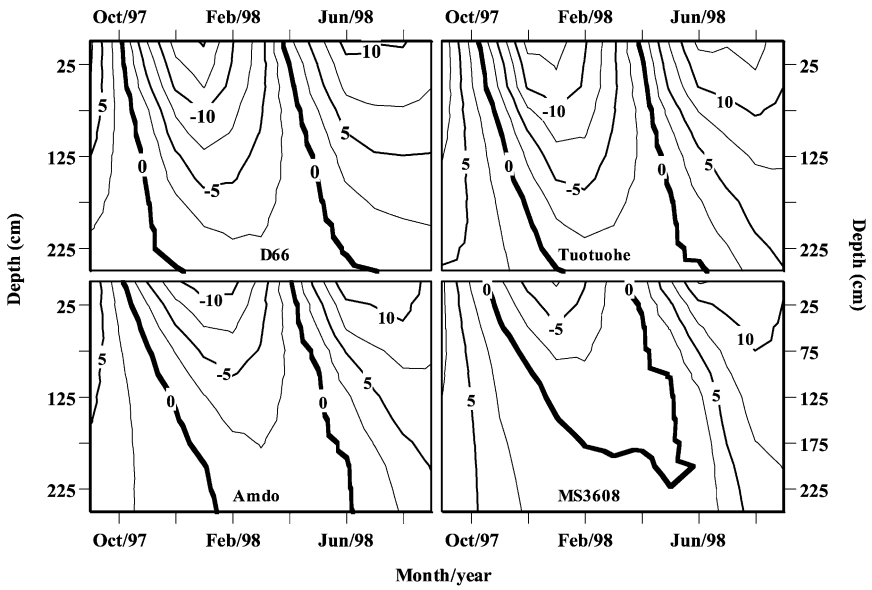

Fig. 2. Contours of ground temperature (°C) at all the study sites on the eastern Tibetan Plateau.

rapidly at D66 and Tuotuohe, where the soils are drier and sparsely covered by grass. The frost front reached 250 cm at D66 in December and at Tuotuohe in January, much earlier than at the other two sites. These differences are surely related to climatic conditions: D66 and Tuotuohe are cold, while the other two sites are relatively warm. They are partially affected by vegetation on the ground surface via its thermal impact on the freezing process. Yabuki et al. (1998) noted such an impact on a small spatial scale. The graph for site MS3608 shows a typical spatio-temporal pattern of soil temperature variation for a discontinuous permafrost underlain region. The 0 °C contour line occurs at a depth of 242 cm, indicating that there is a permanently unfrozen layer between the surface layer, where freezing is seasonal, and a deeper permanently frozen layer.

Fig. 3 shows the spatial-temporal variation in the volumetric soil water content at the study sites. At both D66 and Tuotuohe, the soil became wetter as the ground thawed, and drier as the ground froze. A significant increase occurred after June, which was related to the precipitation caused by the monsoon climate (Table 3). In regions of spatially continuous permafrost (D66, Tuotuohe, and Amdo), the vertical soil moisture variation shows a characteristic profile. Soil moisture decreases from the surface to a depth of about 50 cm; in the layer between 60 and 160 cm, the soil water content is low and there is a low gradient; the moisture increases sharply with depth from 160 to 200 cm. This high gradient definitely indicates an impermeable barrier. This characteristic profile was not as clear at MS3608, where the permafrost was discontinuous. At MS3608, the graph of soil moisture matches the soil temperature contour line over a short interval.

3.2. Water budget and its imbalances

The water budget components in the ground surface layer for the hydrological year September 1997–August 1998 are shown in Table 3 (empty cells denote missing data). Due to the monsoon climate, precipitation occurred predominantly in the summer monsoon period (May–September). Summer precipitation constituted 84% of the annual total at Tuotuohe, and 87% at Amdo. The annual precipitation was 287.0 mm at Tuotuohe and 616.3 mm at MS3608.

Monthly evaporation shows short-term variation related to precipitation events. When the ground starts to thaw in May or June, the monthly evaporation exceeds precipitation. As the thawing front descends, evaporation becomes less than precipitation.

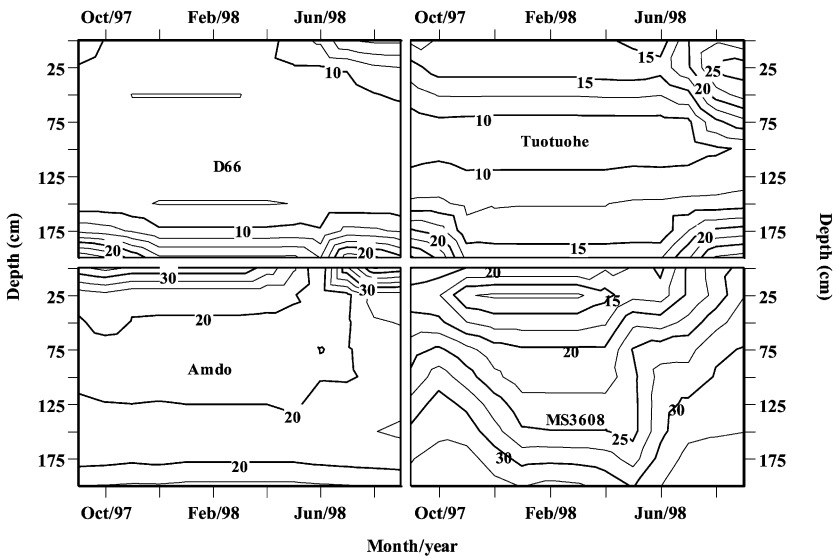

Fig. 3. Contours of the monthly mean soil volumetric water content (%) at all the study sites on the eastern Tibetan Plateau.

Table 3
The water budget calculations for the study sites (unit: mm/month)

Year/month		97/9	97/10	97/11	97/12	98/1	98/2	98/3	98/4	98/5	98/6	98/7	98/8	Total
D66	P_r									7.0	14.8	48.6	48.6	
	E	10.6	2.9	2.0	1.1	2.0	2.1	4.4	4.8	13.2	16.8			
	ΔW	−11.1	−13.5		−0.9	0.0	0.0	0.0	12.2	13.1	5.7	10.8	7.4	7.7
	WF_V	11.1	5.5	1.4	0.0	0.0	0.0	0.0	0.0	0.6	0.2	3.3	2.2	24.3
	Wimb									−19.9	−7.9			
Tuotuohe	P_r	42.2	8.1	7.1	1.0	1.5	6.1	1.5	4.6	14.0	34.8	94.7	71.4	287.0
	E	11.5	6.4	6.7	2.4	8.9	4.7	4.4	9.0	28.6	26.0	22.3	27.4	158.4
	ΔW	22.9	−28.3	−15.2	−0.7	0.0	0.0	0.0	1.8	4.0	−6.5	79.2	54.6	111.8
	WF_V	10.6	12.9	12.7	5.1	0.0	0.0	0.0	0.0	0.1	0.5	2.9	1.1	45.9
	Wimb	−2.7	17.0	2.9	−5.8	−7.4	1.4	−2.9	−6.2	−18.7	14.8	−9.6	−11.7	−29.0
Amdo	P_r	45.2	22.1	8.4	5.6	0.0	3.0	3.6	2.5	0.3	13.5	90.4	152.2	346.8
	E									34.0	47.5	58.6	41.4	
	ΔW	27.3	−16.0	1.5	−3.0	−0.1	0.0	0.0	−49.5	43.7	−7.4	51.8	37.9	86.2
	WF_V	12.2	13.3	9.2	9.9	2.3	0.0	0.0	0.0	0.0	3.0	11.7	14.8	76.4
	Wimb									−77.4	−29.6	−31.7	58.1	
MS3608	P_r	98.8	36.8	10.4	8.4	2.3	2.8	7.1	13.0	3.8	63.8	165.9	203.2	616.3
	E									38.4	73.6	71.9	119.0	
	ΔW	44.6	−10.1	−46.4	−55.0	0.2	2.0	−4.0	20.2	35.4	39.7	42.9	55.5	125.0
	WF_V	6.7	18.9	22.7	24.4	2.9	2.9	1.5	0.0	1.0	5.2	9.4	9.9	105.5
	Wimb									−71.0	−54.7	41.7	18.8	

At all sites, the water storage volume in the soil increased over the year because of a significant increase in precipitation from 1997 to 1998 in the eastern Tibetan Plateau (Sato, 2001).

The vertical water flux (WF_V) at the bottom of the layer over which observations were taken (at depths from 190 to 200 cm) is apparently also influenced by precipitation. In the drier region, the annual WF_V was 24.3 mm at D66 and 45.9 mm at Tuotuohe, but it exceeded 100 mm at MS3608. Although the graphs of the vertical soil moisture profile (Fig. 2) show a positive gradient up to a given layer from deeper layers at all sites except Amdo, WF_V still flows to the deeper layer, since the gradient is not sufficient to exceed gravity forcing. The surface layer consistently loses water to the deeper layers.

The biggest problem in the water budget results shown in Table 3 is the imbalances revealed by the *Wimb* term. The likeliest cause of this problem is lateral water flow that cannot be incorporated in these calculations due to the limited observations. The observation sites were established on flat land, but flat land on the Tibetan Plateau is generally located near the bottom of a valley. As the melt starts, the melting water from surrounding areas, including snow and surface soil, might tend to concentrate at lower places. The incoming water will either evaporate or remain in the lower place, significantly increasing ΔW. This deduction is supported by the large negative value of *Wimb* in May at all of the study sites in Table 3, and is evidenced by the presence of ground water at the beginning of the Monsoon season (Section 2.1). To overcome this failure, it is essential to build a reference site nearby for hydrological investigations in the permafrost region. As Zhang et al. (2000) demonstrated, the existence of permafrost physically limits the subsurface flow system to the thin active layer. subsurface flow, which is the net inflow coupled to soil melting, has been reported on a permafrost slope in a subarctic area (Carey and Woo, 1999).

Such lateral flow may not be simple due to topography, but may also result from heterogeneity of the shallow ground thaw-table. For example, for

a study site near a river (e.g. Tuotuohe), a time lag between the thaw near the river and that at the study site will result from the differences in soil moisture and the presence of river ice. The relative slope of the water table will lead to lateral water flow to the study site. There is no evidence supporting this postulate because we did not examine the spatial distribution of the thaw table in the study region. Such heterogeneity has been reported in the eastern Tibetan Plateau, and is explained by the heterogeneity of surface conditions, such as vegetation (Yabuki et al., 1998).

The deficit in Table 3 may in part be caused by uncertainty in the frozen water content, which is a major barrier to hydrological investigations in permafrost regions. The water content data measured using TDR probes were corrected by assuming that the total frozen water was the same as the water observed the preceding fall, just before the soil froze, and that there was no water input during the frozen period. However, snowmelt has been reported to infiltrate frozen soil (Zhao and Gray, 1999). This infiltration might occur at the beginning and end of the frost season.

A third reason for the imbalance in the water budget seen in Table 3 might be the difficulty of observing precipitation. Systemic errors in snowfall observations are significant in subarctic regions, like Siberia (Yang and Ohata, 2001). The negative values of *Wimb* in winter, which imply that evaporation was not balanced by precipitation, could result from under-catch in the measured precipitation. This error term cannot be corrected either, since there has been no experimental work on correcting gauge-measured precipitation in this region.

4. Analysis

4.1. Evaporation and soil moisture

The calculated daily evaporation at the four study sites is shown in Fig. 4. The obvious seasonal variation in evaporation can be explained by relating it to ground surface conditions, soil thermal processes and precipitation. When the ground surface is frozen

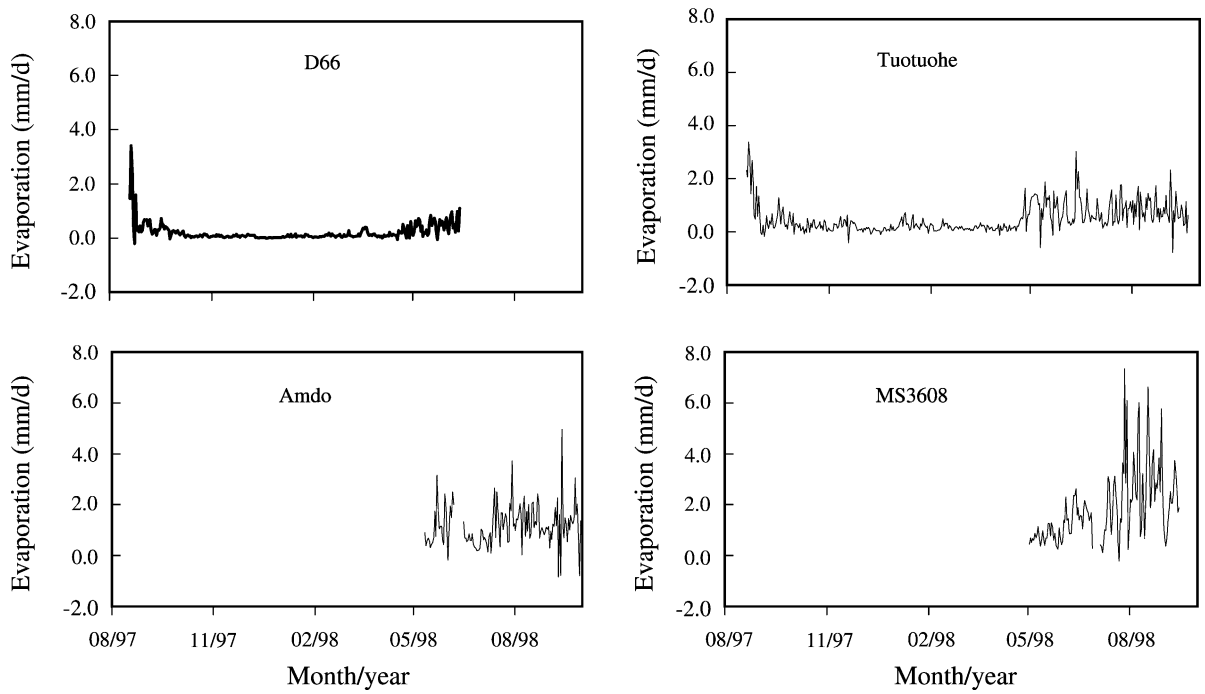

Fig. 4. The calculated daily evaporation at all the study sites.

(October–March), less water leaves the ground surface, since the daily sublimation is less than 0.8 mm. When the ground surface begins to melt (April–May), evaporation increases sharply, which is believed to result from the concentration of melt water within a very thin layer near the surface. When the summer monsoon arrives, evaporation increases with precipitation. After late July, vegetation affects the evaporation via its water-retention capacity. At Tuotuohe, where the vegetation coverage was less than 25%, precipitation rapidly penetrated to the deeper layer—the thawing depth extended beyond 200 cm. At MS3608, where the grass was well developed, the high LAI and dense roots delayed water penetration into the deeper layers, although the impermeable layer is deep here. Additionally, the growing grass led to increased transpiration, resulting in a decrease in evaporation at Tuotuohe after July, but an increase at MS3608.

Evaporation is affected by available energy, near-surface air turbulence, soil water and vegetation. These effects may be partially separated by expressing evaporation as a fraction of its potential value; the ratio of actual evaporation to potential evaporation (E/Ep) is a measure of the extent to which the land surface exerts control over the evaporation process. Ep, the potential evaporation, is given by (Brutsaert, 1984)

$$E\mathrm{p} = \frac{\Delta}{\Delta+\gamma} Q_{\mathrm{ne}} + \frac{\gamma}{\Delta+\gamma} E_{\mathrm{a}} \tag{8}$$

where Δ is the slope of the saturation water vapor pressure curve, and γ is given by

$$\gamma = C_{\mathrm{P}} P / 0.622 L_{\mathrm{e}} \tag{9}$$

where C_{P} is the specific heat of air at constant pressure, P is air pressure, and L_{e} is the latent heat of vaporization of water. Q_{ne} indicates the heat energy available for evaporation, as determined by the net radiation (Q_{n}) and ground heat flux (Q_{g}) :

$$Q_{\mathrm{ne}} = (Q_{\mathrm{n}} - Q_{\mathrm{g}})/L_{\mathrm{e}} \tag{10}$$

E_{a} is a function of wind speed (U) and the saturation deficit ($e_0 - e$) :

$$E_{\mathrm{a}} = 0.26(1 + 0.45U)(e_0 - e) \tag{11}$$

To investigate the dependence of evaporation efficiency on the availability of stored water, the variation of E/E_{p} with surface soil moisture (at 0.04 m) is shown in Fig. 5. It is clear that E/E_{p} increases linearly with ground surface moisture when the volumetric water content is less than 30%, but does not increase with moisture content beyond that level. This stresses the importance of the critical value of soil moisture of 30%. When soil moisture is less than 30%, the evaporation process is restrained by the deficiency of available water. Kondo et al. (1990) noted a similar critical value, and reported that the evaporation efficiency for a loam soil became 1.0 when the soil moisture reached 28%.

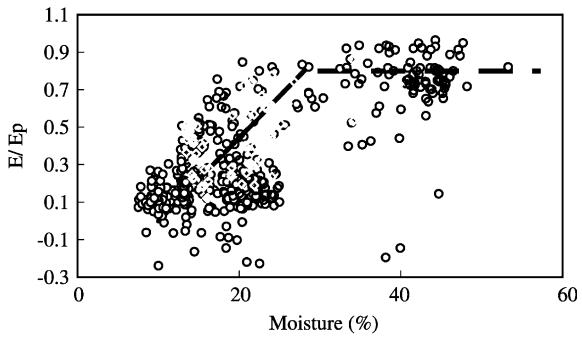

Fig. 5. The ratio of daily evaporation to daily potential evaporation (E/E_{p}) versus surface moisture.

4.2. Changes in water storage and soil moisture

The seasonal variation in water storage in the surface layer and soil moisture measured at the surface and bottom levels at Tuotuohe (continuous permafrost) and MS3608 (discontinuous permafrost) are shown in Fig. 6. As mentioned in Section 2.2, ΔW was calculated from the soil moisture profile, including both liquid and solid water. In the ground surface layer, 0–200 cm for Tuotuohe and 0–190 cm for MS3608, the change in water storage was the most active hydrological component. Its largest daily range exceeded 20 mm/d, which is close to the maximum daily precipitation.

A different pattern of seasonal variation in soil moisture can be seen in the right-hand panels in Fig. 6. At Tuotuohe, a continuous permafrost region, the seasonal variability in soil moisture near the surface and at 200 cm was similar. Both increased as the ground thawed and decreased as it froze, over an

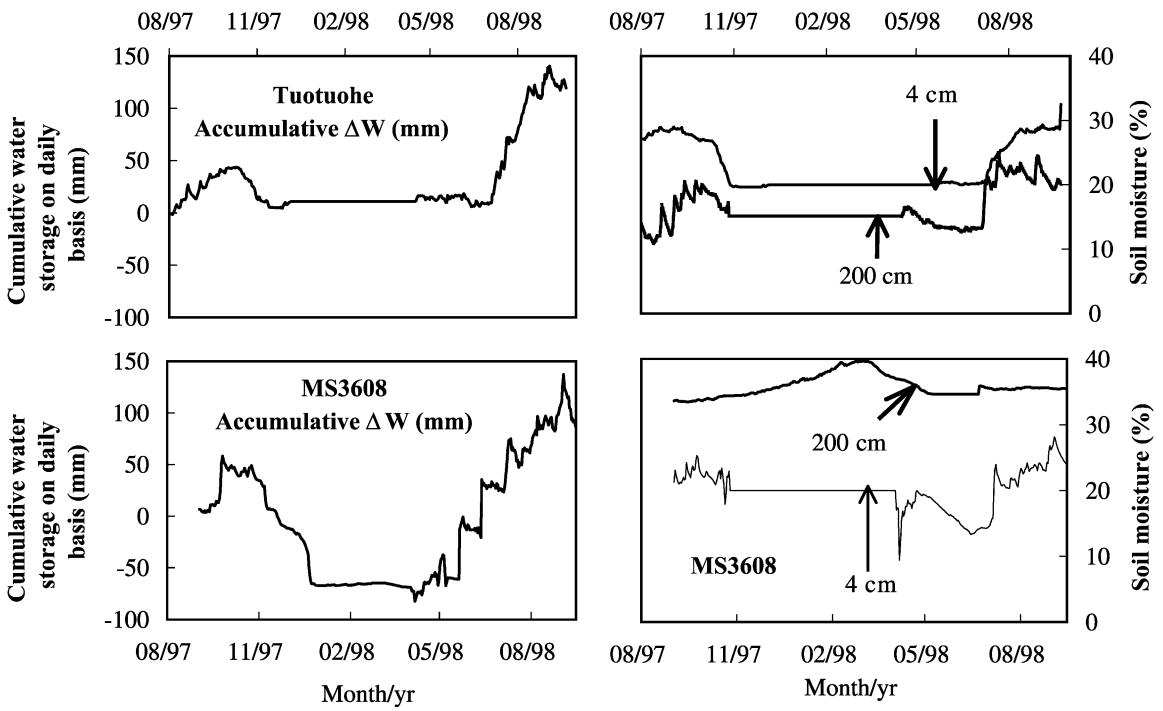

Fig. 6. Seasonal variation in the cumulative daily change in water storage and daily mean soil moisture measured at the surface and bottom of the study layer at Tuotuohe (continuous permafrost) and MS3608 (discontinuous permafrost) on the eastern Tibetan Plateau.

annual range of about 10%. This is exactly the opposite of what happens in discontinuous permafrost regions. Regular variation in the soil moisture was observed at the surface at MS3608, which showed a pattern similar to that at Tuotuohe. At 196 cm depth, however, the soil moisture increased as the ground started to freeze from the surface and reached a peak in late February. This might have been due to increased water at depth due to the freezing process.

The seasonal variation in water storage was similar at the two sites. It is clear that water storage in surface layer increases during the warm period (from soil melt to before freezing), but decreases during the freezing period, October–January. In another words, the soil gets wetter as the lower layers melt, but drier as the upper layer freezes. This tendency is also seen in the monthly values shown in Table 3. The total water storage in the study layer increases since the ground starts melting from the surface. This results from the existence of an impermeable barrier coupled to seasonality in precipitation. The precipitation water penetrates the layer, but cannot go deeper since the bottom of the layer is still frozen. By contrast, when the ground starts to freeze, the water storage decreases since the layer is isolated from the atmosphere and water flows deeper through the unfrozen bottom layers.

Precipitation and evaporation are complementary components of the water balance, the input from the atmosphere, and the return flow from the ground back to the atmosphere. The difference between precipitation (P_r) and evaporation (E) should reflect the change in water stored in the ground surface layer (ΔW); therefore, the value of ΔW must be related to the difference between P_r and E. The variation in ΔW versus ($P_r - E$) at all the study sites in the continuous permafrost region (D66, Tuotuohe, and Amdo) is shown in Fig. 7. The value of ΔW generally increases with ($P_r - E$) along the 1:1 line when $P_r - E$ exceeds zero, which indicates the occurrence of precipitation events. The plots in Fig. 7 are scattered, which may reflect the imbalance terms shown in Table 3 and discussed in Section 3.2. It was not expected that the water stored in the ground surface layer would react linearly to atmospheric forcing, but this may be

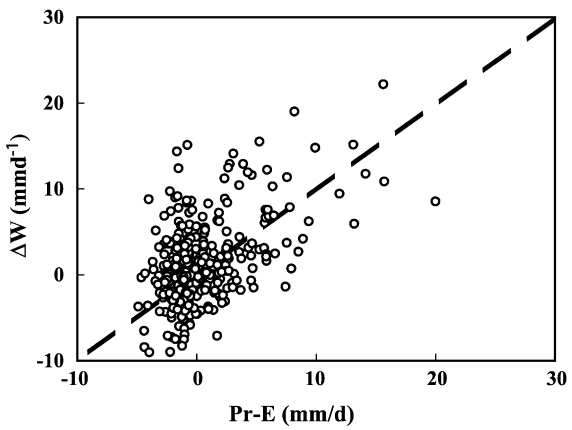

Fig. 7. The daily variation in water storage at 0–200 cm depths (ΔW) versus the difference between daily precipitation and evaporation ($P_r - E$) in a region underlain by permafrost.

related to lateral water flow and other components that were not elucidated in this work.

4.3. Vertical water flux (WF_V)

The amount of water penetrating to the deeper layer (WF_V), which was investigated at a depth of 200 cm in the continuous permafrost region (D66, Tuotuohe and Amdo) and 190 cm in the discontinuous permafrost region (MS3608), is determined by the gradient of the soil-water potential, which can be calculated from the volumetric water content (Fig. 8). Therefore, soil moisture fluctuation, which demonstrates a clear seasonal pattern, will lead to a similar pattern of variation in WF_V. It is certainly influenced by ground thermal conditions, as is obvious in Fig. 2, in which the graphs of data from the continuous permafrost region differ from that obtained in the discontinuous permafrost region (MS3608). The former peaks in the warm season, the latter in December.

The total annual contribution of WF_V to the water budget is also significant. Although the daily value of WF_V is less than 1.0 mm/d, the annual total is 105.5 mm at MS3608 because it is predominantly in one direction. The annual amount of WF_V, clearly influenced by precipitation events, is 24.3 and 45.9 mm at D66 and Tuotuohe, respectively. Both sites are located in a drier region where the annual precipitation is less than 300 mm.

4.4. Water budget and water cycle

Strong seasonality characterizes hydrological processes in the cryosphere. Great contrasts occur between the hydrological state in summer (liquid

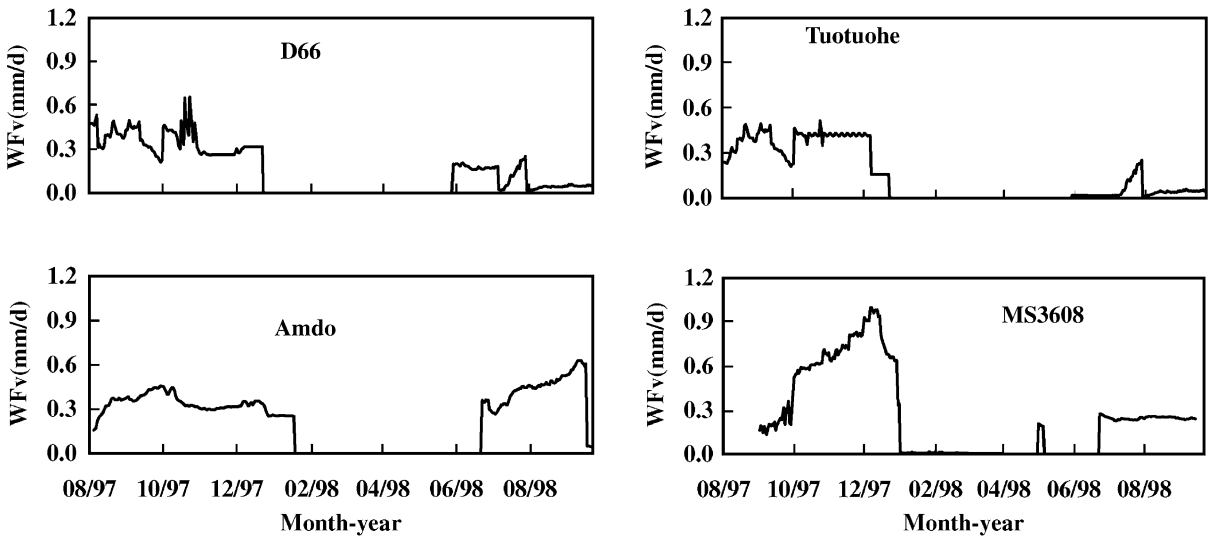

Fig. 8. Seasonal variation in the daily vertical water flux (WF_V) at the bottom of the study layer (200 cm at D66, Tuotuohe, and Amdo, and 190 cm at MS3608).

water) and winter (solid water). In a permafrost-dominated region such as the Tibetan Plateau, permafrost and the active layer control soil moisture and intimately link hydrology to the thermal balance of the soil. The active layer thickness and permafrost conditions are largely controlled by surface heat fluxes, coupling the hydrological process in the ground surface layer (from the surface to 2.0 m depth in this study) to the surface energy budget to the extent that they cannot be quantified separately. Seasonality of the energy budget leads to alternating freezing and thawing of soil. These in turn interact with surface and subsurface hydrological processes, playing different roles at different time scales in the water cycle.

To illustrate the composition of the water budget in annual terms, the example for Tuotuohe is given in Fig. 9, in which the amounts are normalized to a daily time scale to permit comparisons (including the imbalance term *Wimb*). To better understand the significance of hydrological processes in studying the interaction between the ground surface layer and the atmosphere, the hydrological year was divided into several periods according to the seasonal state of the thermal regime in the ground surface layer from the surface to a depth of 200 cm. These were the ground-melting period (April 15–May 27), the period when the whole layer had thawed (May 28–October 26), the ground-freezing period (October 27–December 22), and the period when the whole layer was frozen (December 23–April 14).

In the ground-melting phase, the ground surface layer becomes a system that is open to the atmosphere, but closed to the deeper ground. Precipitation accounts for 100% of the water gain (the imbalance was not included) with a daily mean amount of 0.3 mm/d. Eighty-five percent of the input water was used for evaporation, while 15% stayed in the soil, which significantly increased the soil water content. Evaporation averaged 0.8 mm/d, which exceeded the water input as explained in Section 3.1.

When the surface layer was completely thawed it became an open system, both to the atmosphere and to the deeper soil layers. Precipitation increased to 1.6 mm/d and still accounted for 100% of the water input. Evaporation was reduced to 0.6 mm/d, but ΔW and WF_V were increased to 0.9 and 0.2 mm/d, respectively; they accounted for 37, 53 and 10% of the water loss, respectively. It is perhaps surprising that the evaporation was lower than before, even with a significant increase in precipitation. The increase in the depth of the unfrozen layer, and in precipitation, did not lead to an increase in evaporation as one might expect, but rather reduced it. The explanation may be that the water moved deeper and the water content near the surface was reduced.

When surface freezing started, the active layer became a system that was open to the deeper soil, but not to the atmosphere: there was a little precipitation (0.2 mm/d), which was briefly balanced by upward vapor flow in the form of sublimation amounting to

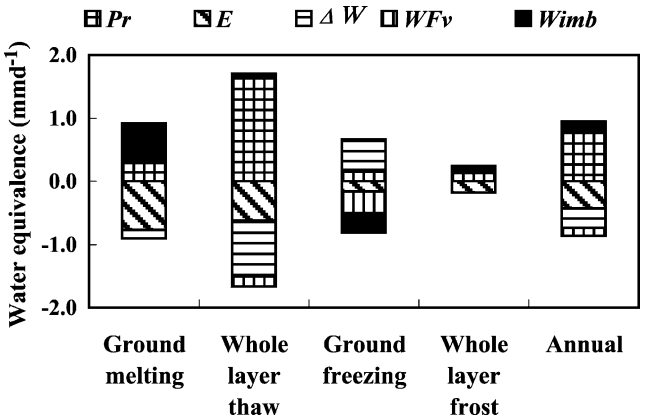

Fig. 9. The composition of the water budget in the ground surface layer (0–200 cm) at Tuotuohe on the eastern Tibetan Plateau.

0.2 mm/d. The dominant hydrological processes occurred in the subsurface layer; WF_V reached 0.3 mm/d, leading to decreasing water storage at a rate of 0.5 mm/d (it did not balance and there was a deficit of 0.2 mm/d). During this period, P_r, E, ΔW and WF_V separately accounted for 26, −32, 74 and −68% of the water budget, respectively. When the active layer was completely frozen, the water cycle almost stopped, except for approximately 14.2 mm of precipitation and 20.7 mm of sublimation.

Precipitation, evaporation, and increasing water storage were the dominant components of the annual water budget of the surface ground layer at Tuotuohe, accounting for 100, −50 and −35%, respectively. Nevertheless, the increase in water storage was related to the increase in precipitation from 1987 to 1988, as mentioned in Section 3.2. Therefore, it is understood that dominant water cycling arises from the processes of precipitation and evaporation, as is typical in this region. On the evidence of a whole hydrological year, the period from the end of May to late October, when the entire layer is thawed, is the most active period for hydrological processes in the ground surface layer.

5. Summary and discussion

The hydrological processes in the surface ground layer of a permafrost region in the Tibetan Plateau were investigated to improve our understanding of the interaction between the atmosphere and permafrost. Data covered the hydrological year September 1997–August 1998, so this study was able to examine seasonal variation in the hydrological processes, but not interannual fluctuation. The monthly mean air temperature and monthly precipitation, measured routinely at the Tuotuohe Meteorological station (WMO ID: 560040) from January 1990 to December 2000 and averaged from AWS data from August 1997 to 1998, are presented in Fig. 10. The annual mean air temperature for the two periods were exactly the same (−3.9 °C), and precipitation averaged 267.5 mm for 1990–2000 and 287.0 mm for September 1997–August 1998. These results indicate that the seasons studied typifying the hydrological components in this climatic regime.

The water regime in the surface ground layer (0–200 cm depth) in the permafrost region of the eastern Tibetan Plateau is predominantly controlled by the development of an active layer of permafrost coupled with the monsoon climate. The temporal synchronicity of the increase in precipitation and melting ground surface results in precipitation water penetrating to the soil, increasing water storage. In the process of soil freezing, the water storage decreases, since the soil is isolated from the atmosphere, but water still flows to the deeper layers through the unfrozen lower layers. Water storage in the surface layer is very variable, and is sensitive to precipitation and evaporation. The total water storage in the shallow 2 m surface layer exhibits regular seasonal variation related to the seasonality in precipitation. Similar seasonality in the soil moisture is seen near the surface (60 cm depth) throughout the study region, but it is opposite in the deeper layers in the continuous and discontinuous permafrost regions.

At the onset of the ground surface melt, the concentration of melt water within a rather thin surface layer leads to a rapid increase in evaporation. This evaporation is reduced when the wet soil zone moves downwards. A decrease in evaporation in August and September is found in the continuous permafrost region, with short-term variation coupled to precipitation events. Similar seasonality of evaporation has been reported in Trail Valley Creek, a continuous permafrost region in Canada (Rouse, 2000).

In both the continuous and discontinuous permafrost regions, the vertical water flux, which ranged from 25 to 105 mm annually, was not negligible. It reduced the water storage when the surface was frozen but the deeper soil was not. Interestingly, that annual vertical water flux equaled the same fraction of the annual precipitation in both the continuous and discontinuous permafrost regions (Tuotuohe and MS3608) with values of 16 and 17%, respectively, despite the fact that the annual precipitation differed markedly.

The freeze–thaw cycle, which affects seasonal soil moisture, water storage, evaporation, and the assembly of water via the soil and vegetation during the summer monsoon season, is a dominant feature of the land-surface hydrology in the permafrost region of the eastern Tibetan Plateau. The contributions of precipitation and evaporation to the water budget demonstrate that the precipitation–evaporation mechanism

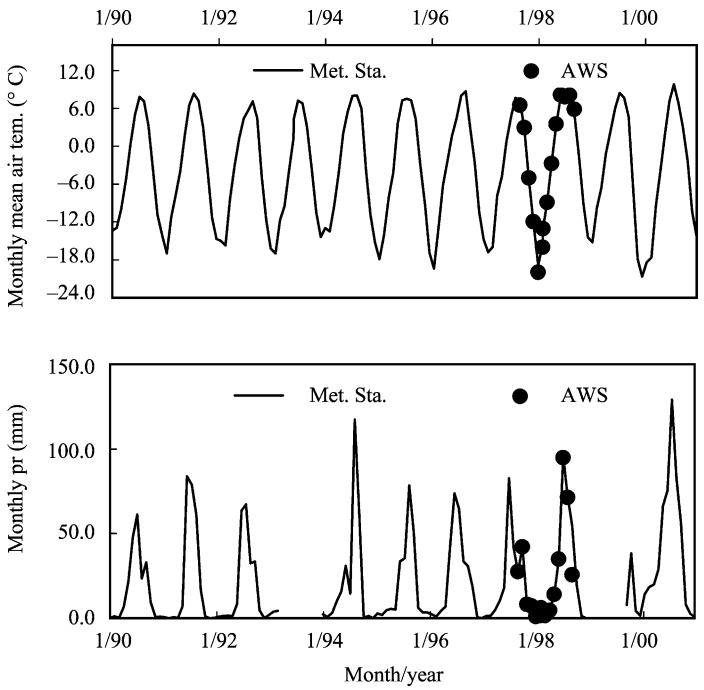

Fig. 10. Monthly mean air temperature and monthly precipitation measured at the meteorological station and at AWS for Tuotuohe from 1990 to 2000.

is the dominant process in the water cycle, at both local and regional scales.

Compared with other permafrost regions, one of the characteristics of the study region is that snow cover is irregularly and discontinuously distributed over the ground surface, even in the middle of winter (Sato, 2001). At Tuotuohe, the precipitation during the period when the ground surface is frozen (October 27–May 14) was 25 mm, while the evaporation was 30 mm. The role of snow cover in the surface hydrological process was not as significant as reported in North America or Siberia (Woo and Winter, 1993; Ma et al., 1998).

This study investigated land-surface hydrological processes on a unidimensional basis. Some shortcomings of this study, like the water budget imbalance, necessitate more detailed work in this area. Special attention should be paid to the hydrological features in permafrost regions, including the possible significance of lateral water flow, the heterogeneity of shallow ground, and the under-catch in snowfall observations. Additionally, better calibration of the TDR probe used to measure soil moisture is an absolute prerequisite in order to obtain a reasonable estimate of the water budget.

Acknowledgements

All of the data used in this paper were from the GAME/Tibet POP and IOP projects. We would like to thank everyone who took part in the observation programs. The authors also thank the Frontier Observational Research System for Global Change (FORSGC) of Japan for supporting the work involved in preparing this paper.

References

Barnett, T.P., Dumenil, L., Schlese, Roeckner, 1988. The effects of Eurasian snow cover on global climate. Science 239, 504–507.

Brutsaert, W., 1984. Evaporation into the atmosphere, Reidel, Dordrecht, pp. 197–231.

Carey, S.K., Woo, M.-K., 1999. Hydrology of two slopes in subarctic Yukon, Canada. Hydrol. Process. 13, 2549–2562.

Hahn, D.G., Shukla, J., 1976. An apparent relationship between Eurasian snow cover and Indian monsoon rainfall. J. Atmos. Sci. 33, 2461–2462.

Koike, T., 2000. Summary Report of GAME/Tibet Program, The 2nd Session of the International Workshop on TIPEX-GAME/Tibet.

Kondo, J., Xu, J., 1996. An estimation of heat balance for arid and semi-arid region in China. 1. climatological conditions, soil parameters and calculation method. J. Jpn Soc. Hydrol. Water Resour. 9, 162–174.

Kondo, J., Saigusa, N., Sato, T., 1990. A parameterization of evaporation from bare soil surfaces. J. Appl. Meteor. 29, 385–389.

Kukla, G.J., Kukla, H.J., 1974. Increased surface albedo in the Northern Hemisphere. Science 183, 709–714.

Lawford, R.G., 1993. The role of ice in the global water cycle. IAHS Publ. 214, 151–161.

Li, G., Duan, T., Haginoya, S., Chen, L., 2001. : Estimation of the bulk transfer coefficients and surface fluxes over the Tibetan Plateau using AWS data. J. Meteorol. Soc. Jpn 79 (2), 625–635.

Liu, C., Wang, H., 1999. The interface processes of water movement in the soil–crop–atmosphere system and water-saving regulation, Chinese Science Press, pp. 82–85.

Ma, X., Hiyama, T., Fukushima, Y., Hashimoto, T., 1998. A numerical model of the heat transfer for permafrost regions. J. Jpn. Soc. Hydrol. Water Resour. 11 (4), 346–359.

Nagai, H., Kobayashi, T., Ishikawa, H., Teshima, J., 2002. An analysis of soil moisture and evaporation at a grassland station of GAME/Tibet Amdo using the BBH model. J. Jpn. Soc. Hydrol. Water Resour. 55 (1), 3–12.

Rouse, W.R., 2000. Progress in hydrological research in the Mackenzie GEWEX study. Hydrol. Process. 14, 1667–1685.

Sato, T., 2001. Spatial and temporal variation of frozen ground and snow cover in the eastern Tibetan Plateau. J. Meteorol. Soc. Jpn 79, 519–534.

Stone, P.H., Quirr, W.J., 1977. The July climate and a comparison of the January and July climates simulated by the GISS general circulation model. Mon. Wea. Rev. 29, 652–657.

Sugimoto, A., Tanaka, K., Ichiyanagi, K., Kurita, N., Yamazaki, T., Kotake, T., Kubota, J., Yanagiasawa, N., Argovkin, Y., 2001. Spatial and seasonal variations in surface soil moisture around Yakutsk observed in 2000. Proc. GAME-Siberia Workshop, GAME Publ. 30, 63–73.

Tanaka, K., Ishikawa, H., Tamagawa, I., 2001. Surface energy budget at Amdo on the Tibetan Plateau using GAME/IOP 98 data. J. Meteorol. Soc. Jpn 79, 505–517.

Williams, J., 1975. The influences of snow cover on the atmospheric circulation and its role in climate change: an analysis based on results from the NCAR global circulation model. J. Appl. Meteorol. 14, 137–152.

Woo, M.K., Winter, T.C., 1993. The role of permafrost and seasonal frost in the hydrology of northern wetlands in North America. J. Hydrol. 141, 5–31.

Woo, M.K., Xia, Z., 1996. Effects of hydrology in the thermal conditions of the active layer. Nord. Hydrol. 27, 129–142.

Xu, J., Haginoya, S., 2001. An estimation of heat and water balances in the Tibetan Plateau. J. Meteorol. Soc. Jpn 79, 485–504.

Yabuki, H., Seko, K., Ageta, Y., 1998. Estimate of the depth of the active layer in the permafrost region of the Tibetan Plateau on satellite images. J. Jpn. Soc. Hydrol. Water Resour. 11, 253–259.(in Japanese with English abstract).

Yang, D., Ohata, T., 2001. A bias-corrected Siberian regional precipitation climatology. J. Hydrometeorol. 2 (2), 122–139.

Zhang, Z., Kane, D.L., Hinzman, L.D., 2000. Development and application of a spatial-distributed Arctic hydrological and thermal process model. Hydrol. Process. 14, 1591–1611.

Zhao, L., Gray, D.M., 1999. Estimating snowmelt infiltration into frozen soils. Hydrol. Process. 13, 1824–1842.

Zhou, Y., Guo, D., Qiu, G., Cheng, G., Li, S., 2000. Geocryology in China, Science Press China, pp. 299–360.